УДК 539.1.074.55

SILICON TWO-COORDINATE DETECTOR WITH SEPARABLE PAD-STRIP READOUT

L.S.Barabash, A.V.Babookh, V.N.Frolov, M.Yu.Kazarinov, A.A.Popov, V.G.Sandukovsky, V.V.Tchalyshev
Joint Institute for Nuclear Research, Dubna, Russia

A.Wang
University of Maryland College Park MD, USA

The characteristics of resistive layer Si microstrip detector with two versions of the readout system are presented. One version used the usual single coordinate strip system of 1 mm pitch. The second version used a two coordinate pad-strip system of 3.6 mm pitch («chess board»). The registration precision of the detector was studied with a UV laser. The two-dimensional imaging ability of the detector with α-particles and with an ^{241}Am γ-source is shown.

The investigation has been performed at the Laboratory of Nuclear Problems, JINR.

Кремниевый двухкоординатный детектор с внешней пэд-стриповой системой считывания

Л.С.Барабаш и др.

Приводятся характеристики Si микростripового детектора с резистивным слоем. Для испытаний детектора применялись две различные версии считывающей системы: обычная однокоординатная стриповая система с шагом стрипов 1 мм и двухкоординатная система с электродами (пэдами) размером $3,6 \times 3,6$ мм^2, расположенными в шахматном порядке. Точность регистрации координат определялась с использованием ультрафиолетового лазера. Показаны двумерные образы, полученные методом облучения детектора α- и γ-частицами.

Работа выполнена в Лаборатории ядерных проблем ОИЯИ.

1. Introduction

The creation of semiconductor detectors with two-dimensional imaging has important application for clinical diagnosis in nuclear medicine as well as for experimental nuclear physics. Simulations of the *X*-ray sensitivity of semiconductor detectors indicate a high efficiency for photon registration in the 25-60 keV range of clinical interest [1]. Using a detector geometry with a sandwich structure of 0.5 mm silicon wafers for an overall sandwich thickness of 4—5 mm can further increase the registration efficiency to near 0.2 for 60 keV photons. A disadvantage of this detector geometry is that the number of

electronic channels rises in proportion to the detector area. The photon registration efficiency can also be increased by the use of high ohmic pure silicon crystals or lithium-doped silicon (Si(Li) crystals) [2]. It is possible in these cases to create silicon detector having an effective thickness of 4—5 mm with a reasonable base voltage and fewer electronic channels.

This article describes the investigation of a silicon detector suggested in [3]. The detector uses a pad-strip system which allows measurements of two-dimensional images with only a moderate number of electronic channels and a relatively simple level of manufacturing technology.

2. Detector Layout

The detector consists of a flat diode manufactured by the surface-barrier technology from silicon with specific resistance equal to 2.5 $k\Omega \cdot$ cm (Fig.1). Rectifying contacts are created by a layer of gold (50 $\mu g/cm^2$), deposited on a surface of n-Si crystal. An undepleted layer of silicon is used as the anode and is grounded in one or two points. The detector has dimensions of 10×30 mm^2 and a thickness of 0.2 mm.

The sensitive electrode system was manufactured on printed circuit board and was placed on the anode side of detector, and isolated from the anode by a 30 mm mylar film. Each element of the coordinate system (pads of strips) was connected to the input of a charge sensitive amplifier. The signals from amplifier output went to the ADC (LeCroy 2248A). The conversion gain of the charge sensitive amplifier was 2.5 V/pC. The noise levels of separate electronic channels during the 1 msec ADC strobe pulse were 4—6 keV.

The signals from the output of one of the amplifier channels was used to generate a trigger pulse and the electronic registration threshold was (0.5—0.7) fC.

The amplitude caliboration and the estimation of the electronics noise level were normalized by the falling edge of the gamma spectrum from a ^{241}Am gamma source.

Two cooridnate system were used for registration of the charge distributions on the resistive layer: a usual one-dimensional strip system with pitch of strips $S = 1$ mm; and a two-dimensional pad-strip system (laid out as a chess board) with a distance between the pad centers of $S = 3.6$ mm.Pads were joined into strips as shown in Fig.1 and each strip

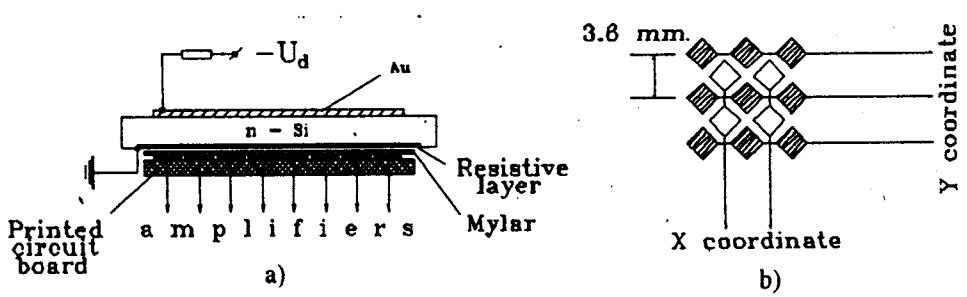

Fig.1. a) The layout of semiconductor detector; b) scheme of the pad-strip readout system

connected to a charge sensitive amplifier input. Event cooridnates in the pad-strip system were calculated from the registered charge distribution projected along two orthogonal axes.

Eight electronic channels were used during the investigations. When using the one-dimensional strip system, it was possible to register the event coordinates from a 8×10 mm^2 area. In the two-dimensional version we used 4 channels for registration of each coordinate, the event coordinates were registered from a 120 mm^2 area of the detector.

3. Precision of Event Registration in Detector

The precision of event registration was studied using a UV pulsed nitrogen laser. The laser ray was collimated by a 20×30 μm^2 collimator and was normal to the surface of the detector. The intensity of the laser ray was changed widely by a set of mylar films. A sliding table shifted the detector relative to the laser ray with a precision of 10 μm.

The detector was not completely shielded from inductances created by the power laser high voltage generator. Consequently, the level of noise entering the electronic channels was greater by a factor of 3, than the noise level in the measurements with the redioactive sources.

The measured registration precision σ of the collimated UV laser beam position is shown in Fig.2 for a one-coordinate strip system with pitch of strips equal to 1 mm. The registered charge amplitude Q is presented in arbitrary units. The charge amplitudes corresponding to the falling edge of a ^{241}Am gamma source are shown by arrows and are equal to 500 arbitrary units.

The same measurements for a two coordinate pad-strip system with pitch 3.6 mm are shown in Fig.3. The registration precision was calculated from the coordinates of the charge amplitudes pojected along one of the orthogonal axes. Curve 1 shows the dependence of the detector precision on the projected charge amplitude for coordinates calculated by the center of gravity, and curve 2 obtained by fitting the projected charge distributions with a Gaussian function.

Figures 4a and 4b show the results of simulating the expected detector registration precision σ as a function of the strip pitch S. Both σ and S are normalized to the r.m.s. of the charge distributions σ_{cd}. The simulations were done for different levels of electronic channels noise σ_n. The relative level of noise is shown at the right column of the figure as the ratio

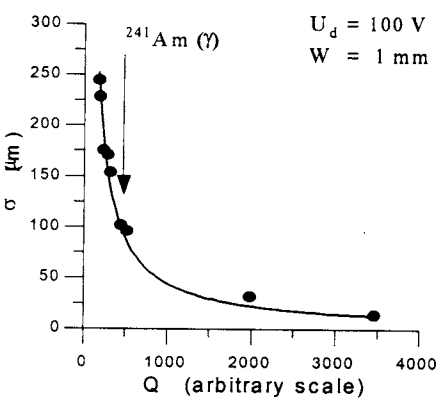

Fig.2. Dependence of the precision of detector on the amplitude of the registered charge for one coordinate readout with pitch of strips $S = 1$ mm

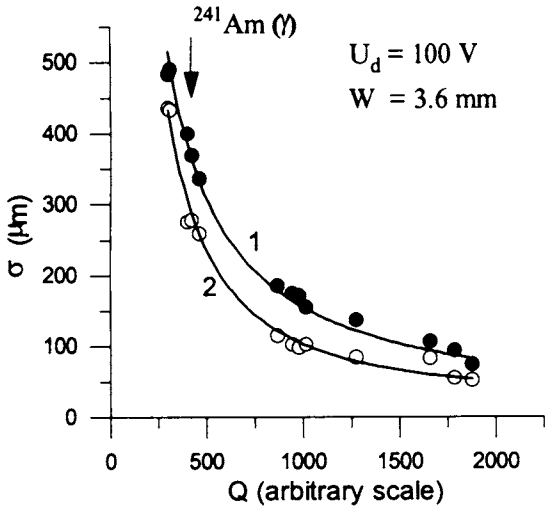

Fig.3. Dependence of the precision of the detector on the amplitude of registered charge for two coordinate pad-strip system with $S = 3.6$ mm. 1 — for coordinates calculated by the center of gravity, 2 — for the use of Gaussian fit

σ_n / Q_{max}. For a given value of S, the charge Q registered during a single event was calculated as the integral of the charges deposited in each strip. It was assumed that the shape of charge distributions were Gaussian. The errors of the charge amplitude measurements were normalized to the central strip amplitude Q_{max}.

Figure 4a shows events which hit the center of the strips. As is seen from the figure, the best precision can be realized for S approximately equal to $1.5 \cdot \sigma_{cd}$ and increases with higher noise levels. Figure 4b shows events which occur in the gaps between the strips. For the events hitting between the strips the detector precision σ approaches some limiting value, which occurs when the total charge distribution is registered by two strips only and the ratio σ_n / Q_{max} is minimal.

Figures 4a and 4b demonstrated that there is a systematical change of detector registration precision for any given width of strips S. The precision σ is minimal for between strip events and maximal for central strip events, and the amplitude of the systematical oscillations increases with the increase of strip width.

The error of the total charge measurement can be written by formula:

$$\sigma_Q = a\sigma_n .$$

The coefficient $a = 1/n$, where n is the number of strips used for the calculation of the event coordinate by the center of gravity method, and σ_n is the error determined by the noise of the electronic channels. As the results of the simulation show, the value of coordinates calculated by fit equals 1.5 approximately.

The results of this simulation show that the error in the coordinate calculation depends on the ratio σ_n / Q_{max}, so that realization of a low level of electronic channel noise is a very important requirement for this kind of detector. Even the realization of a noise ratio of order 0.1 would allow a factor of 5—10 reduction in the number of electronic channels in the data acquisition system in comparison with a usual strip semiconductor detector operating at the same coordinate resolution.

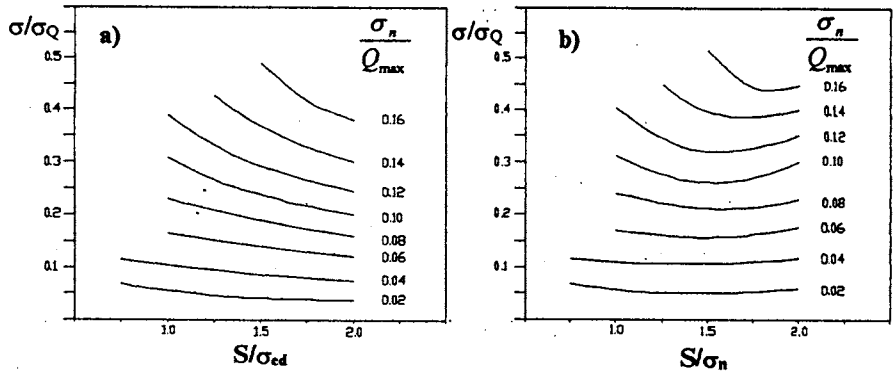

Fig.4. Results of simulation of detector precision for different pitch of strips S and for different level of electronic channel noise, a) for central events, b) for between strip events

4. The Width of the Charge Distributions

The width of the charge distributions, registered by the sensitive electrode system, is determined by product RC_d, where R is the surface resistance of the underleted silicon layer and C_d is the capacitance per unit of detector area [4].

The measured dependence of the charge distribution width σ upon the detector base voltage U_d is shown at the top of Fig.5. The bottom curve comes from previously measuremed unpublished data for a detector manufactured from silicon of specific resistivity $13k\Omega \cdot$ cm [3]. As is seen from the figure, both curves have a saturation area. It means, that both the resistance and the thickness of the undepleted silicon layer become independent of the base voltage after the saturation point and are constant. This region corresponds to the deep depleted detector. Calculation of the undepleted silicon thickness for an assumed Gaussian charge distribution gives a value equal to (6—10) μm for both types of silicon. Naturally, the specific capacitance of the detector does not change under this condition.

Thus, both the lower bound on the range of σ_{cd} and the registration precision σ of this kind of detector are constrained by the undepleted zone, and further increase of the precision should be obtained with high ohmic silicon.

As can be seen from Fig.5, the limiting width of the charge distribution for 13 $k\Omega \cdot$ cm silicon is 0.3 mm and 0.66 mm for 2.5 $k\Omega \cdot$ cm silicon.

An additional criterion for rejection of noise pulses is the requirement that the charge distribution must be registered in a cluster of adjacent strips. Further analysis of the shape of the registered charge distributions provided a very strong and effective method for rejection of noise pulses.

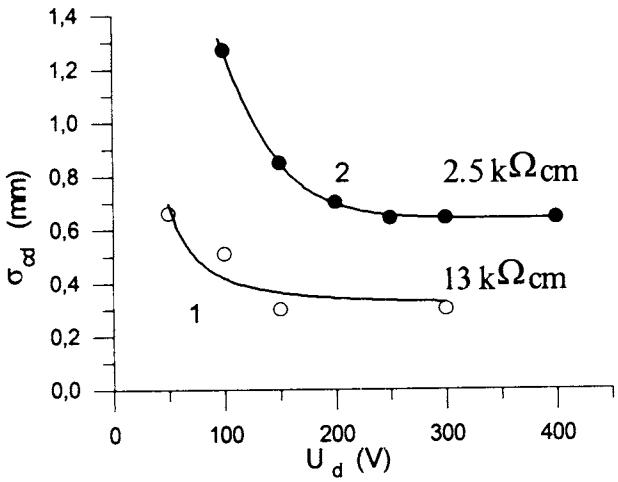

Fig.5. Dependences of the charge distribution width (r.m.s.) shaped on the resistive layer from the base voltage of detector for different specific resistances of silicon

V. Imaging Ability of Detector

The imaging ability of the detector was checked with phantoms placed on the detector surface. Two-coordinate pad-strip system of sensitive electrodes with 3.6 mm pitch was used for registration of the images.

Figure 6 shows the measurement of the position of a straight piece of Cu wire with diameter of 0.5 mm oriented along one coordinate of the detector. The detector was irradiated by a collimated α-particle beam from a ^{239}Pu radioactive source, with all measurements performed in air to maximize the energy loss. In order to study the dependence of the imaging quality on the total charge amplitude of the registered distributions, the energy of α-particles was varied by changing the distance from detector to radioactive source. Figure 6a shows the spectra of α-particles detected at different distances. The size of the collimator hole was adjusted for different spectra so that the coordinate error from the ultimate size of the beam would not exceed 30—50 μm.

The cross sections of the phantom images along the coordinate orthogonal to the wire is shown in Fig.6 (b,c,d,e). Event coordinates were calculated for charge amplitude intervals corresponding to spectra 1,2,3 and 4 of Fig.6a, respectively. It is obvious that the phantom is recognized quite well even for spectrum 1. The precision of detector was better than for the laser investigation (see Figure 3). It can be explained by the lower level of noise, which was less by factor 3, as noted above.

Figure 7 shows the results of measurement of position of a phantom obtained in the beam from ^{241}Am gamma source. A piece of solder with diameter of 1 mm oriented along

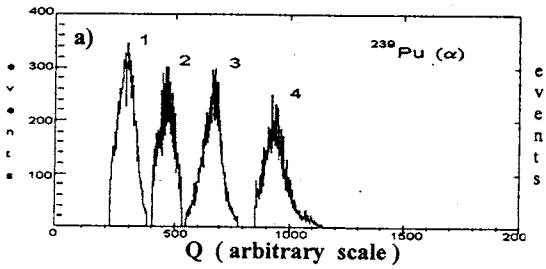

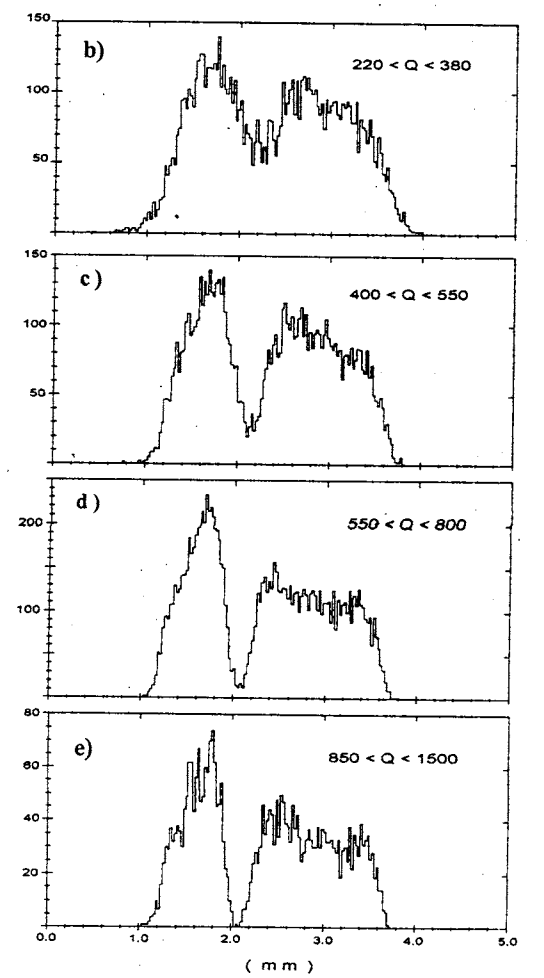

Fig.6. a) The amplitude spectra of α-particles for different distances between the detector and the ratio active source. b), c), d), e) The cross-sections of phantom images for different amplitude spectra

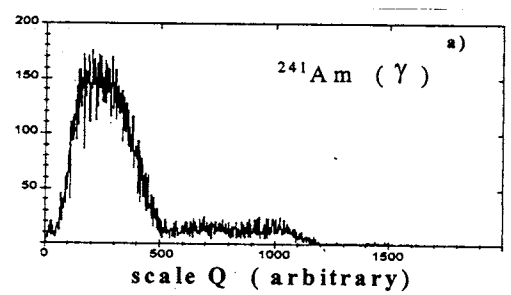

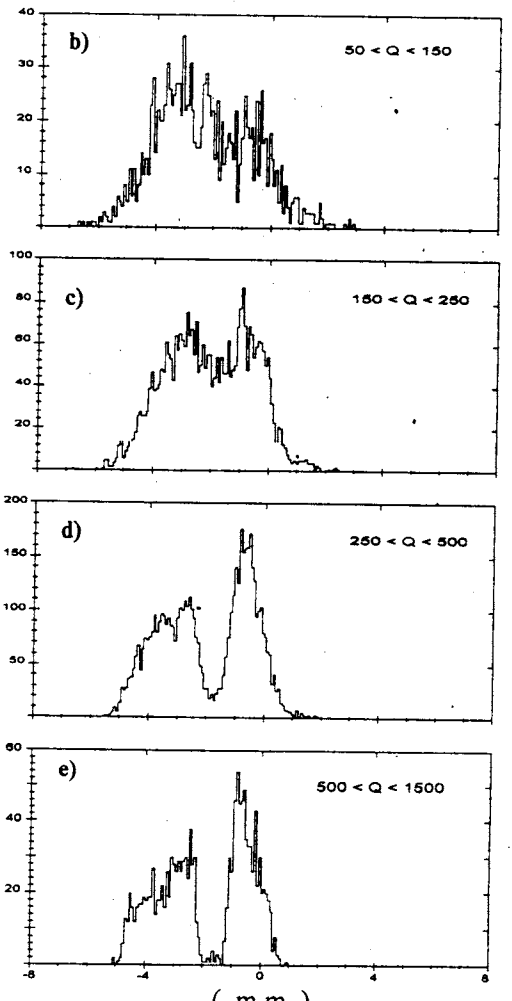

Fig.7. a) The amplitude spectrum obtained with the ^{241}Am gamma source. b), c), d), e) The cross sections of the phantom image for different intervals of amplitude spectrum

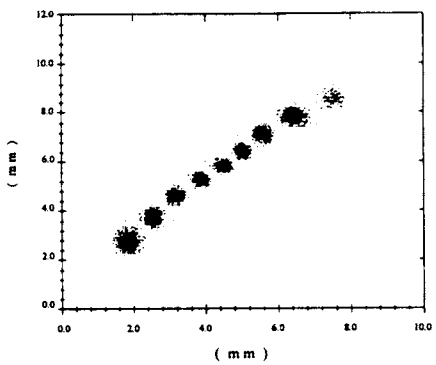

Fig.8. Calibration plot obtained by the use of the collimated UV laser beam for pad-strip readout system with $S = 3.6$ mm

one of the coordinates was used as the phantom. The spectrum of registered charge distributions is shown in Fig.7a. The tail of the spectrum is determined by the alpha particles which passed through the shielding film of the source. The cross sections of the phantom are shown on Figs.7 (b,c,d,e), which were obtained for different intervals of amplitude of charge. As is seen from the Figure, the energy resolution is not sufficient for separation of 59.6 keV line, but it is enough for obtaining coordinate resolutions of the order of (100—150) μm.

The calibration plot obtained in the UV laser beam for the signal amplitudes corresponding to spectrum 3 of Fig.6a is shown in Fig.8. The distance between different positions of the beam is equal to 1 mm. The value of the systematical error in the calculated coordinates for the central range of detector was 0.93 along both coordinates and was taken into account for both projections of the event coordinates. The origin of this systematical error arises from the limitation of having only four electronic channels available for calculation of each coordinate.

Figure 9 illustrates the imaging ability of the detector with a complex phantom. The external phantom was a 2 mm open circle made of 0.32 mm diameter Cu wire. A flat tin drop with diameter of 0.5 mm was used as the internal phantom. The third phantom placed

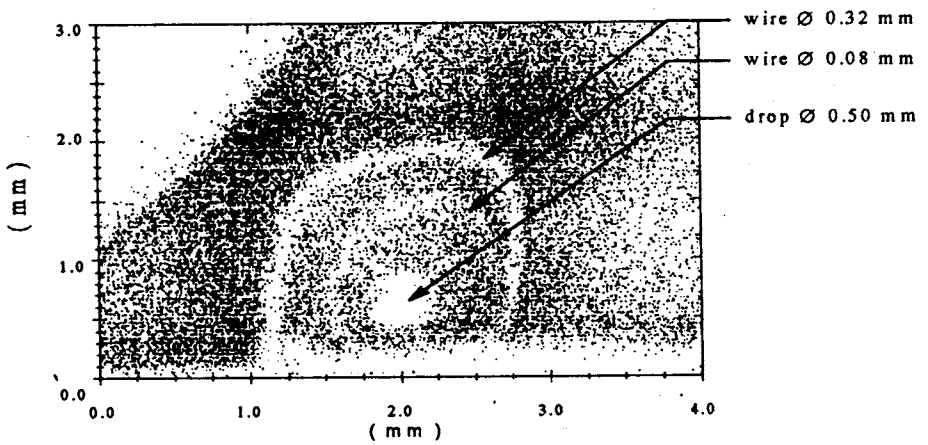

Fig.9. Images of different phantoms obtained by the use of the α-particle beam and pad-readout system with $S = 3.6$ mm

between the external and internal phantoms was a 1.8 mm open circle produced of 80 microm diameter Cu-Be wire.

The phantom images were obtained in a beam of α-particles with energy corresponding to spectra 4 of Fig.6a. The image was cut off at the bottom by the condition of the trigger. Measurements were done for the base voltage of detector $U_d = 100$ V. As can be seen from the picture, the precision of the detector is less than 50 μm in spite of the quite large pitch between the centers of the sensitive electrodes (3.6 mm). The width of registered charge distribution (σ_{cd}) equals 1.3 mm for this base voltage and the ratio S/σ_{cd} is 2.76. This ratio and the required number of electronic channels used for rigistration of the charge distribution information determine the origin of the systematical errors of the calculated coordinates which deform the imaging of phantoms.

Conclusion

In conclusion we would like to mark some advantages of the semiconductor detector scheme described here.

It allows the realization of two-coordinate readout from detectors of simpler technology in manufacture than the usual two-side strip detector technology.

Both the simulation results and the laboratory investigation of this kind of detector show that it is possible to obtain good coordinate resolution even with quite large distances between the readout electrodes.

Analysis of the shape of the resitered charge distributions provides highly effective rejection of the noise pulses.

Suggested pad-strip system allows a significant reduction in the number of electronic channels in comparison with the usual pad readout systems.

The detector scheme suggested here is applicable to the production of large area semiconductor detectors. The possible area of the detectors is limited only by the size of the silicon wafers.

Acknowledgement

We would like to thank A.F.Novgorodov for the preparation of the radioactive sources used for investigation and useful discussions of obtained results.

One of the authors would like to acknowledge support from the Texas National Research Laboratory Comission while at the University of Maryland.

References

1. Bencivelli W., Bertolucci E., Bottigli U. et al. — Nucl. Instr.&Meth., 1991, A-305, p.574.
2. Biebl U., Parak F. — Nucl. Instr.&Meth., 1973, v.112, p.455.

3. Barabash L.S., Tchalyshev V.V. — Semiconductor Position Sensitive Detector, 1985, N1181405 USSR; Discoveries and Inventions, 1990, v.24, p.273, (in Russian).
4. Barabash L.S., Belcarz E., Gurov Yu.B. et al. — Nucl. Instr.&Meth., 1990, A-288, p.375.
5. Barabash L.S., Mesaross L., Rchalyshev V.V. — JINR Communications, R13-86-563, Dubna, 1986 (in Russian).

Received on February 5, 1996.